Interferometer for phase-stabilization of quantum nodes using SIL-based color centers

Koek, Wouter D.; Hagen, Ronald A.J.; Vaselli, Margherita; Morits, Jaco P.J.; Stolk, Arian J.; van der Enden, Kian L.; Benjamin Biemond, J. J.; van Zwet, Erwin J.; Croese, Jared; More Authors

DOI
10.1117/12.3023175

Publication date
2024

Document Version
Final published version

Published in
Quantum Computing, Communication, and Simulation IV

Interferometer for phase-stabilization of quantum nodes using SIL-based color centers

Wouter D. Koek*[a,b], Leon van Dooren[a], Ronald A.J. Hagen[a,b], Hedser van Brug[a], Margherita Vaselli[a,b], Jaco P.J. Morits[a,b], Arian J. Stolk[b,c], Kian L. van der Enden[b,c], J.J. Benjamin Biemond[a,b], Erwin J. van Zwet[a,b] and Jared Croese[a,b]

[a]Netherlands Organisation for Applied Scientific Research (TNO), 2628 CK Delft, The Netherlands ; [b]QuTech, Delft University of Technology, 2628 CJ Delft, The Netherlands ; [c]Kavli Institute of Nanoscience, Delft University of Technology, 2628 CJ Delft, The Netherlands

ABSTRACT

Many quantum entanglement generation protocols require phase stabilization between the nodes. For color centers that are embedded in a solid immersion lens (SIL) often a reflection from the SIL's surface is input to an interferometer where it is mixed with a reference beam. However, the beam reflected beam by the SIL does not travel colinear with the photons that are emitted by the color center, which ultimately leads to a reduction of the interferometer's signal-to-noise ratio (SNR). Additionally, imperfections of the SIL surface introduce aberrations into the reflected light, thereby further reducing the SNR. Through several design-iterations and extensive experience realizing phase stabilization on many different SIL's we have come to an approach that significantly improves the SNR and enhances the operability of the quantum node. In this paper we report on our optical design and provide useful guidelines for the operation thereof.

Keywords: quantum entanglement, phase stabilization, solid immersion lens, interferometer, birefringent crystals, beam steering, interference contrast, patterned aperture, smart aperture

1. INTRODUCTION

To enable the future quantum internet it is required to generate remote entanglement between distant quantum nodes[1]. The performance of such a quantum link is determined, amongst other things, by the entanglement rate and thus depends on the efficiency with which photons can be collected from the qubit. The use of a solid immersion lens (SIL) enhances the collection efficiency of zero phonon line (ZPL) photons that are emitted by a color center[2].

A promising approach to realizing a multimode quantum network requires phase stabilization between the nodes, where this phase stability can be realized by implementing a number of phase control loops[3]. In a proven successful approach a "local" and a "global" interferometer are used in conjunction to implement phase stability[3].

As shown in Figure 1, in the local interferometer the phase difference between a (higher-power) reference beam, hereafter referred to as stabilization light, and the readout (i.e. excitation) beam reflected from the SIL is typically measured. Subsequently this phase difference can for example be controlled by adjusting the phase of the RF-signal that is driving the acousto-optic modulators (AOM's), thereby compensating mechanical vibrations and other sources of phase error at the node. It is important to note that the stabilization light is *also* used for the global interferometer, and thus (along with the ZPL photons) needs to be coupled into the optical fiber link that connects to a remote node or midpoint. In order to minimize the phase error due to misalignment between the stabilization light and the ZPL beam, it is important that these beams are aligned to be nominally colinear. This however has direct consequences for the alignment of the beams in the local interferometer.

As also shown in Figure 1, due to manufacturing tolerances the color center is typically not located directly underneath the SIL's apex and thus, in order to maximally illuminate the color center, the readout beam will be slightly decentered with respect to the SIL. Consequently the SIL reflected light will propagate in a different direction than the ZPL photons.

*wouter.koek@tno.nl

Quantum Computing, Communication, and Simulation IV, edited by Philip R. Hemmer, Alan L. Migdall, Proc. of SPIE Vol. 12911, 129111F · © 2024 SPIE
0277-786X · doi: 10.1117/12.3023175

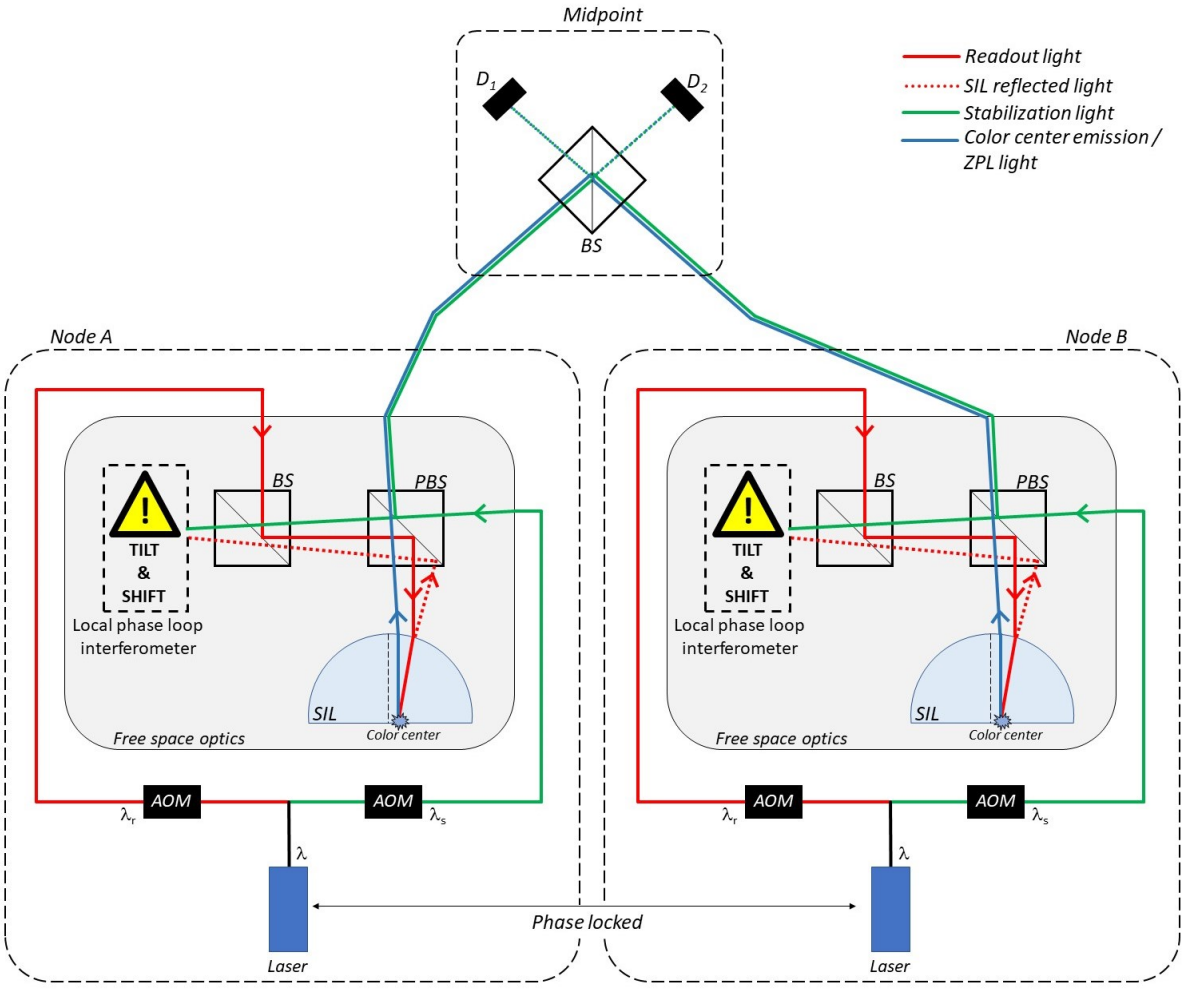

Figure 1. Highly simplified layout of a phase-stabilized multimode quantum network, illustrating the practically unavoidable tilt and shift between the two beams entering the local interferometer.

Because the stabilization light has been aligned to propagate colinear to the ZPL photons this means that the beams that enter the local interferometer have an angular mismatch. Due to the propagation distances involved the beams may also experience a significant spatial shift.

If the AOM's are operated at different frequencies, the wavelength of the SIL reflected light (λ_r) is slightly different from that of the stabilization light (λ_s), and a heterodyne interferometer is formed. It has been long known that the signal to noise ratio (SNR) of a heterodyne interferometer is subject to the relative shift and tilt of the interfering beams[4], or more general, that it depends on the complex overlap integral between both beams[5]. Because the SNR of the heterodyne beat signal may effectively limit the accuracy with which the relative phase difference between both beams can be determined[6], it is imperative that considerations to improve the complex beam overlap play a crucial role in the optical design of the local interferometer.

2. OPTICAL DESIGN TO IMPROVE COMPLEX BEAM OVERLAP

As shown in Figure 2, in the optical design of the local interferometer we implemented dedicated functionality to mitigate the relative tilt and shift of the beams, as well as a generic (yet flexible) means to combat residual aberrations

thereby (further) improving the modulated power in the heterodyne beat signal. We will discuss both functionalities separately.

2.1 Tilt and shift mitigation

As can be deduced from the beam paths through the polarizing beam splitter (PBS) in Figure 1, the SIL reflected light and stabilization light are orthogonally polarized. Although one might be tempted to first separate the beams using their orthogonal polarization, and then subsequently overlap them after the tilt and shift have been corrected by adjusting a set of mirrors in either one of the beam paths, this would introduce a non-correctable non-common path error. Instead, the tilt and shift need to be corrected in a common path approach.

When using birefringence as a steering mechanism the orthogonally polarized beams can be given different tilts and/or shifts while traversing the same optical components. Beam steering solutions based on birefringent crystals and liquid crystals arrays have previously shown to work well[7]. Since in the here discussed application the tilt and shift corrections are a one-time SIL-specific "set-and-forget" adjustment we prefer the use of (static) birefringent crystals over an active liquid crystal device, as the latter might require control loops of its own.

As can be seen in Figure 2, upon entering the local interferometer the beams go through a first set of a half wave plate (HWP) and a birefringent component. This first birefringent component serves to correct the relative tilt and is composed of two birefringent wedges, where the wedge angle and the direction of the optical axes of both wedges have been carefully designed to meet the required angular correction range and resolution. Note that the birefringent component can be rotated around two axes. Since the relative tilt will be induced in the plane that is spanned by the optical axes of the two birefringent wedges, the rotation along the (nominal) optical propagation direction serves to set the *orientation* of the tilt correction. It is quite practical if the HWP is made to rotate along since this keeps the polarizations of the incoming beams aligned with the main axes of the birefringent crystals when the latter is rotated. The other rotation, effectively rotating the optical axes of the two birefringent wedges in the plane in which tilt is induced, sets the *magnitude* of the relative tilt.

Next the beams traverse a second set of HWP and a birefringent component: this serves to correct the relative shift between the beams. The shift corrector consists of a single birefringent slab for which the thickness and the direction of the optical axis has been carefully chosen to meet the required lateral shift range and resolution. Like with the tilt corrector, the crystal can be rotated around two axes to set the direction and magnitude of the relative shift between the two beams.

Now that the relative tilt and shift between the two beams has been minimized, the beams enter the next part of the interferometer.

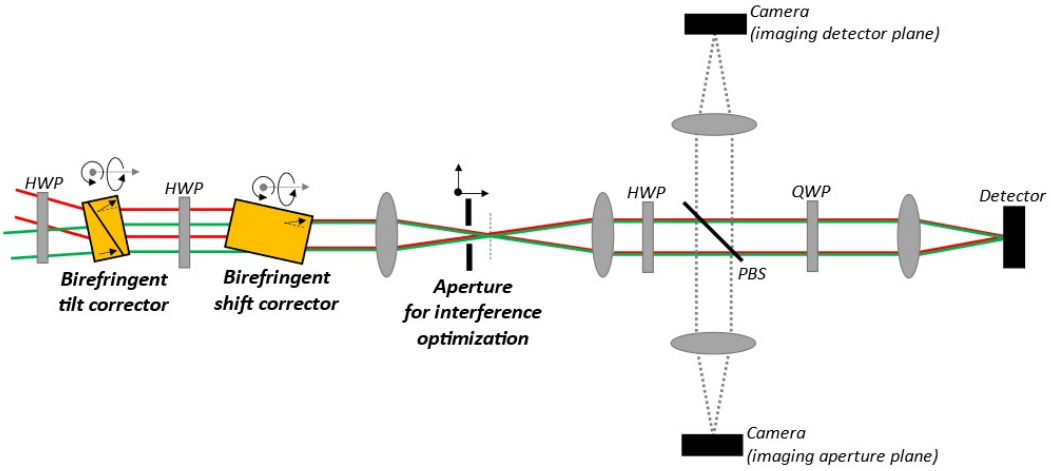

Figure 2. Schematic optical layout of an interferometer that uses birefringent crystals to ensure beam overlap, and an aperture to optimize modulated power onto the detector

2.2 Residual aberrations mitigation, optimization of modulated power

Although we have implemented a dedicated means to mitigate relative tilt, tilt is only one of many aberrations that can occur. Other aberrations, when left uncorrected, will also negatively affect the complex beam overlap and thus the amount of modulated power in the interferometric beat. It is important to realize that other than in Section 2.1 where the overall complex overlap integral between the SIL reflected and stabilization light was improved, in this Section we merely aim to mitigate the negative impact of the residual aberrations. The part of the interferometer that consists of the two lenses with the intermediate aperture serves this purpose (Fig. 2). This is accomplished by first focusing the beams to form a beam waist, next transmitting only a selected portion of the overlapping wavefronts *around* (i.e. not necessarily *in*) the beam waist to reduce the negative impact of the aberrations on the modulated power of the beam that will reach the detector, and finally re-collimating the beam for further processing and transport to the detector.

Note that aberrations *itself* are actually not a concern, the main concern here lies in *unshared* aberrations between both beams. For example, if both beams have the *same amount* of spherical aberration this will not negatively affect their ability to produce optimal interference contrast. If they have a different amount of spherical aberration then the relative phase difference between the beams will show up as a central lobe with surrounding rings of alternating phase. Although the beams will *interfere* all over their area of spatial overlap, the heterodyne beat at the central lobe will be out of phase with certain rings and in phase with other rings. Since the positive beat contribution of an in-phase ring will be cancelled out by a neighboring out-of-phase ring the effective modulated power in the beat is determined by the area of the central lobe, meaning the least amount of defocus between both beams would (obviously) be preferred. There are however other considerations why one may choose to position the color center (slightly) underneath the SIL center, meaning that the beams entering the local phase loop typically have different spherical aberration.

Unshared aberrations may also occur due to shape errors in the SIL manufacturing process. In order to further illustrate the impact and mitigation of aberrations Figure 3(a) shows a simulated phase difference between two beams. Figure 3(b) highlights regions where this phase difference is less than $\pi/2$ radians relative to the phase difference in the center of the beams. These yellow regions effectively identify areas in which the local phase of the heterodyne beat is such that it contributes positively to the modulated power that would be obtained if only a small centered section of the beams would be transmitted. The overall effect of transmitting these additional "similar phase" regions obviously depends on the amount of power that is contained in them, and should be weighed against the complexity of a patterned aperture.

Based on the aforementioned examples it becomes apparent that, compared to an unfiltered beam, using a single circular aperture with an appropriately chosen diameter may (significantly) improve the modulated power of the transmitted beam. Additionally, a more patterned (i.e. zoned) aperture may further improve the modulated power.

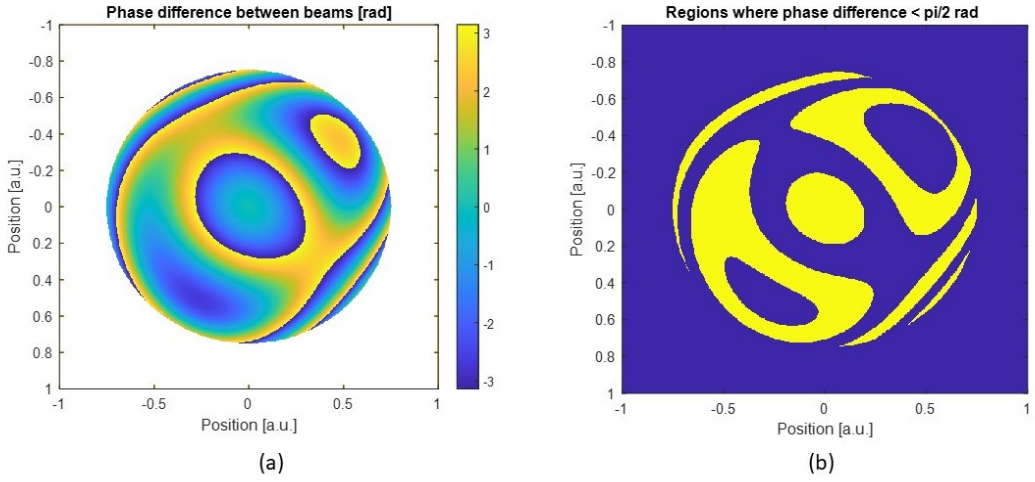

Figure 3. (a) Simulated phase difference between two simulated beams. (b) Yellow areas indicate regions where the phase difference is less than $\pi/2$ radians relative to the phase difference in the center of the beams.

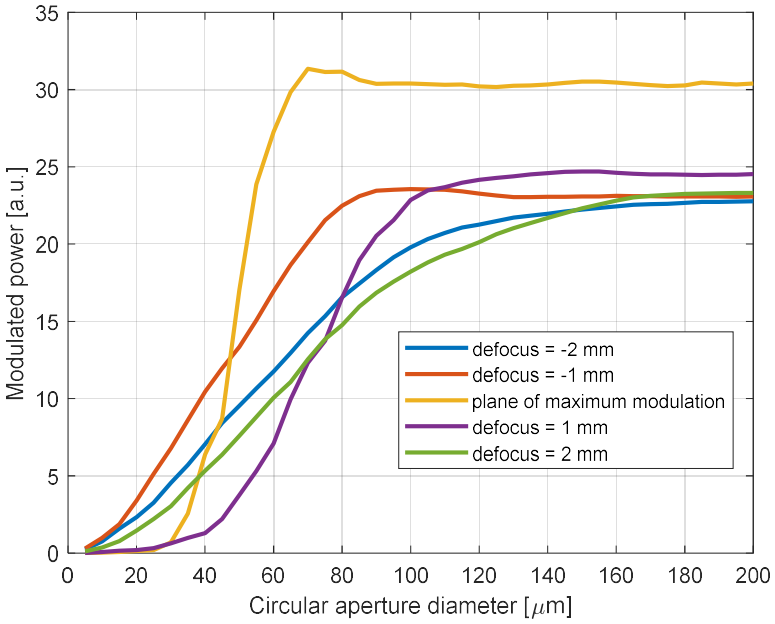

Figure 4. Simulated modulated power onto the detector for circular apertures with varying diameter at various positions around the beam waist (based on measured through focus camera images).

Obviously the optimal shape and size of the aperture is different for each node, and highly SIL-specific. This is why we have equipped our interferometer with the ability to image the overlapping beams in and around the beam waist. As can be seen in Figure 2, after the beams pass the aforementioned spatial filter they encounter a half wave plate (HWP) and polarizing beam splitter (PBS). This combination serves to distribute adjustable ratios of the SIL reflected light and the stabilization light to the detector and the bottom camera, and to ensure that in each of these paths the polarizations of both beams (that were hitherto orthogonal) are made parallel so that they can produce power modulation upon interference. The camera can be scanned through a space that is conjugate to the aperture space. If the aperture is removed, and the AOM frequencies are set such that a beat is formed that can be properly sampled given the camera's framerate, then the camera can be used to determine the spatially resolved modulated power and the phase thereof in and around the beam waist. This measured data can then be used to select the proper shape, size and position of the aperture.

Figure 4 shows an analysis that was performed on such measured data. Here the dataset was analyzed for finding the optimal diameter and position for a circular pinhole aperture. It was found that a properly positioned ∅ 70 µm pinhole produces the largest amount of modulated power. However, using the dataset also sensitivity analyses can be performed (e.g. how sensitive the modulated power is to misalignments or drifts of the pinhole position). Eventually for this particular node we chose to place a ∅ 100 µm pinhole in the plane of maximum modulation.

Note that the camera subsequently allows for easy alignment of the aperture. First the camera is set to observe the plane of maximum modulation. Next the pinhole can be inserted and while it is illuminated from the back, the pinhole can be brought into focus and laterally positioned until it transmits the preferred region of the wavefront.

2.3 Other functionalities

We have now discussed most components that are shown in Figure 2. What remains to be discussed are the beam paths going to the right and upward from the PBS.

In order to properly measure the heterodyne beat, which is typically chosen to be in the MHz regime, a sufficiently fast (and thus small) photodetector is required. Since the diameter of the detector is typically smaller than that of the incoming beam a lens is used to focus the light in order to underfill the detector's active area. Note that although Figure

2 shows a single detector on one of the exit ports of the PBS, it is possible to use both exit ports (i.e. also the path leading to the camera) for detection of the beat, e.g. using a balanced detector. Depending on the detector configuration the HWP will need to be adjusted to optimize the SNR of the beat, which does not necessarily correspond to the setting where the strongest beat power is observed.

The quarter wave plate (QWP) in the detector path does not affect the detected signal, but serves to direct light that is reflected from the detector towards the upper camera. This not only suppresses unwanted reflections back into the node, but using the camera the alignment of the focused spot onto the detector can be easily checked and optimized if needed.

3. DISCUSSION AND CONCLUSION

We have implemented the here presented design on various quantum nodes using a variety of different SIL's and find that it works very well. Compared to earlier nodes we are reaching a better SNR under otherwise comparable circumstances, and have found that the available metrology helps to facilitate and improve alignment, debugging and periodic inspection.

In the current design the optimization of modulated power is done by spatial filtering of the beam. Even with the use of the aforementioned patterned apertures still light, i.e. potential contribution to the beat, is filtered out. Such removal of light can be avoided if the unshared aberrations are to be corrected by means of a phase aperture instead of an amplitude aperture. We consider this to be a possible future improvement. A polarization-dependent spatially-varying phase plate, can be made using a patterned birefringent element. The patterned birefringent element can be tailor made (e.g. using metamaterials) based on measurements using the camera system, or it can be an actively adjustable element (e.g. liquid crystal device). Either way, such an element could either be positioned in or around the beam waist, but also in the collimated beam (in which case the lenses around the aperture can be removed). If the latter is done, and the decision has thus been made to include an active optical element in the local interferometer, then it becomes quite attractive to consider also using this for the tilt correction as described in Section 2.1. We have yet to gather practical experience with the use of liquid crystal devices in the local interferometer, and will report on the feasibility and trade-offs thereof in the future.

At QuTech we not only perform ground-breaking quantum experiments, but we are also committed to the continuous improvement of the critical modules that enable these experiments. By improving the performance of these modules, or by making them more robust or easier to operate, we are helping to pave the path towards the future quantum internet. In this paper we discussed how the iterative improvement of one such module, the local interferometer, has led to a design that works very well in practice. If you are interested in how our expertise can be of use to you, please contact the author.

REFERENCES

[1] H. Kimble, "The quantum internet," Nature **453**, 1023–1030 (2008).
[2] W. Pfaff, *et al*, "Unconditional quantum teleportation between distant solid-state quantum bits", Science **345**, 532 (2014).
[3] M. Pompili, *et al*, "Realization of a multinode quantum network of remote solid-state qubits," Science **372**, 259-264 (2021).
[4] T. Takenaka *et al*, "Signal-to-noise ratio in optical heterodyne detection for Gaussian fields," Applied Optics **17**, 3466 (1978).
[5] https://www.rp-photonics.com/optical_heterodyne_detection.html
[6] D. Rife and R.R. Boorstyn, "Single-Tone Parameter Estimation from Discrete-Time Observations," IEEE Transactions of Information Theory **20**, 591 (1974).
[7] P.F. McManamon *et al*, "Review of Phased Array Steering for Narrow-Band Electrooptical Systems," Proceedings of the IEEE **97**, 1078-1096 (2009).